Accepted Manuscript

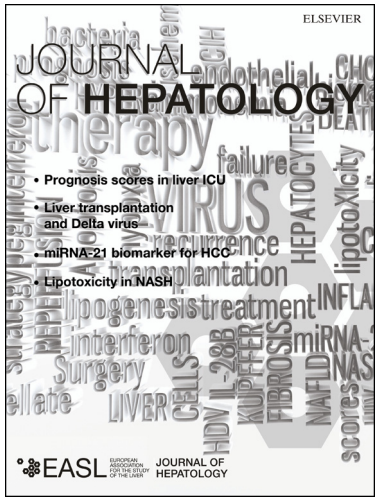

Distinct miRNA signatures associate with subtypes of cholaganiocarcinoma from infection with the tumorigenic liver fluke *Opisthorchis viverrini*

Jordan L. Plieskatt, Gabriel Rinaldi, Yanjun Feng, Jin Peng, Ponlapat Yonglitthipagon, Samantha Easley, Therawach Laha, Chawalit Pairojkul, Vajarabhongsa Bhudhisawasdi, Banchob Sripa, Paul J. Brindley, Jason P. Mulvenna, Jeffrey M. Bethony

PII: S0168-8278(14)00382-1
DOI: http://dx.doi.org/10.1016/j.jhep.2014.05.035
Reference: JHEPAT 5187

To appear in: *Journal of Hepatology*

Received Date: 14 March 2014
Revised Date: 7 May 2014
Accepted Date: 21 May 2014

Please cite this article as: Plieskatt, J.L., Rinaldi, G., Feng, Y., Peng, J., Yonglitthipagon, P., Easley, S., Laha, T., Pairojkul, C., Bhudhisawasdi, V., Sripa, B., Brindley, P.J., Mulvenna, J.P., Bethony, J.M., Distinct miRNA signatures associate with subtypes of cholaganiocarcinoma from infection with the tumorigenic liver fluke *Opisthorchis viverrini*, *Journal of Hepatology* (2014), doi: http://dx.doi.org/10.1016/j.jhep.2014.05.035

Distinct miRNA signatures associate with subtypes of cholangiocarcinoma from infection with the tumorigenic liver fluke *Opisthorchis viverrini*

Jordan L. Plieskatt[1,2*], Gabriel Rinaldi[1,2,3*], Yanjun Feng[1,2], Jin Peng[1,2], Ponlapat Yonglitthipagon[4], Samantha Easley[5], Therawach Laha[7], Chawalit Pairojkul[8], Vajarabhongsa Bhudhisawasdi[8], Banchob Sripa[8], Paul J. Brindley[1,2*], Jason P. Mulvenna[4,9*], Jeffrey M. Bethony[1,2*†]

1. Department of Microbiology, Immunology & Tropical Medicine, School of Medicine & Health Sciences, The George Washington University, Washington, DC 20037 USA
2. Research Center for the Neglected Diseases of Poverty, School of Medicine and Health Sciences, George Washington University, Washington, DC 20037 USA
3. Departamento de Genética, Facultad de Medicina, Universidad de la República, (UDELAR), Montevideo 11800, Uruguay
4. Infectious Disease and Cancer, Queensland Institute for Medical Research, Brisbane, Australia.
5. Department of Pathology, School of Medicine and Health Sciences, George Washington University, Washington, DC
6. Department of Pharmacology & Physiology, School of Medicine & Health Sciences, The George Washington University, Washington, DC 20037 USA
7. Department of Parasitology, Khon Kaen University School of Medicine, Khon Kaen, 40002, Thailand
8. Faculty of Medicine, Khon Kaen University, Khon Kaen, 40002, Thailand
9. School of Biomedical Sciences, Faculty of Medicine and Biomedical Sciences, University of Queensland, Brisbane, Australia.

*These authors contributed equally to this work.

† Corresponding author

Correspondence:

Jeffrey M. Bethony

Department of Microbiology, Immunology and Tropical Medicine,

School of Medicine & Health Sciences,

George Washington University, Washington DC, 20037,

USA; fax +1 202 994 7499; email, jbethony@gwu.edu

Electronic Word Count: Abstract-250, Body/References-4,392, Figure Legends-329

Figures/Tables: Two tables, Four Figures, One supplementary file

Key words:

MicroRNA, cholangiocarcinoma, intrahepatic cholangiocarcinoma, histological grade, *Opisthorchis viverrini,* microarray

Abbreviations:

CCA: Cholangiocarcinoma

ICC: Intrahepatic cholangiocarcinoma

HCC: hepatocellular carcinoma

FFPE: Formalin Fixed Paraffin Embedded

FC: Fold Change

OV: *Opisthorchis viverrini*

miRNA: microRNA

qPCR: Quantitative Reverse Transcription PCR

GWU: George Washington University

IRB: Institutional Review Board

CTT: (intrahepatic) cholangiocarcinoma Tissue

D-NT: Distal Non-Tumor tissue

N-NT: Normal Non-Tumor tissue

ANOVA: Analysis of Variance

CC: Correlation Coefficient

PCA: Principal Components Analysis

Author Statement: The authors report no conflict of interest. The contents are solely the responsibility of the authors and do not represent the official views of NIAID, NCI, the Katzen Cancer Research Center of the George Washington University, or the NHMRC of Australia. This research was partially supported by awards R01CA155297 (JMB, JPM, and PJB) from the National Cancer Institute, P50AI098639 (BS, JMB, and PJB) from the National Institute of Allergy and Infectious Disease, fellowship support (JPM) and research support (JMB and JPM) from the National Health and Medical Research Council of Australia, and research support from the Dr. Cyrus And Myrtle Katzen Cancer Research Center at the George Washington University (PJB and JMB).

Abstract (245)

Background: Intrahepatic cholangiocarcinoma (ICC) is a significant public health problem in East Asia, where it is strongly associated with chronic infection by the food-borne parasite *Opisthorchis viverrini* (OV). We report the first comprehensive miRNA expression profiling by microarray of the most common histologic grades and subtypes of ICC: well differentiated, moderately differentiated, and papillary ICC.

Methods: MicroRNA expression profiles from FFPE were compared among the following: ICC tumor tissue (n = 16), non-tumor tissue distally macrodissected from the same ICC tumor block (n =15), and normal tissue (n =13) from individuals undergoing gastric bypass surgery. A panel of dysregulated miRNAs was validated by qPCR.

Results: Each histologic grade and subtype of ICC displayed a distinct miRNA profile, with no cohort of miRNAs emerging as commonly dysregulated. Moderately differentiated ICC showed the greatest miRNA dysregulation in quantity and magnitude, followed by the papillary subtype, and then well differentiated ICC. Moreover, when ICC tumor tissues were compared to adjacent non-tumor tissue, similar miRNA dysregulation profiles were observed.

Conclusions: We show that common histologic grades and subtypes of ICC have distinct miRNA profiles. As histological grade and subtypes are associated with ICC aggressiveness, these profiles could be used to enhance the early detection and improve the personalized treatment for ICC. These findings also suggest the involvement of specific miRNAs during ICC tumor progression and differentiation. We plan to use these insights to (a) detected these profiles in circulation and (b) conduct functional analyses to decipher the roles of miRNAs in ICC tumor differentiation.

INTRODUCTION

Intrahepatic cholangiocarcinoma (ICC) is an adenocarcinoma which arises in the bile ducts within the liver [1] and is subcategorized morphologically as mass-forming, periductular-infiltrating, or intraductal [2]. ICC is a serious public health problem in East Asia, especially in the Mekong River Basin countries of Thailand, Laos, Cambodia, and Vietnam [3-5], where the incidence of this tumor is the highest in the world (96 per 100,000) [3-5]. This is due to ICC's strong association with chronic infection by the food-borne liver fluke *Opisthorchis viverrini* (OV) [6], one of three eukaryote pathogens considered Group 1 carcinogens by WHO's International Agency for Research on Cancer [6]. Health disparities in this resource-poor region exacerbate mortality by OV-induced ICC because of either (a) suboptimal or nonexistent screening programs and (b) few resources for cancer treatment once a tumor is detected [7]. As OV-induced ICC tends to present late, the prognosis is often poor, with a median survival rate of less than 24 months [8-10]. Hence, the urgent need for biomarkers for improved early detection of OV-induced CCA [11].

Currently, tumor location and stage are the primary prognostic tools for ICC [8]. The WHO suggests a quantitative grading system for ICC tumor differentiation based on the proportion of gland formation [1]: well-differentiated tumors exhibit greater than 95% gland formation, moderately differentiated tumors exhibit between 50% to 95% gland formation, and poorly differentiated tumors exhibit between 5% to 49% gland formation. ICC can also undergo a secondary form of malignant transformation, as a papillary type adenocarcinoma [1]. Due to the late presentation of ICC and the need for re-sectioned liver sample, histology is seldom used in the prognosis or in the planning of patient treatment for ICC, even though moderately differentiated and papillary ICC are generally related to a poor outcome [11, 12]. As such, a biomarker in an accessible bodily fluid such as serum or urine, which could detect ICC prior to liver resection, would greatly aid current prognostic and planning methods for this cancer.

MicroRNAs (miRNAs) are key players in the control of numerous physiological and pathological processes during carcinogenesis, including cellular transformation, tumor differentiation, neoplastic proliferation, and apoptosis [13]. Altered expression of miRNAs has also been reported in other forms of hepatocellular carcinomas (HCC), where a strong correlation between miRNA dysregulation and histological differentiation of the tumor has been observed [14-17]. As miRNAs are well-preserved after formalin fixation, there has been a surge of interest in their development as biomarkers in retrospective cancer studies using FFPE as presented in the current manuscript [13].

Although previous reports have focused on single miRNAs involved in the oncogenesis of OV-induced ICC (e.g.,[16, 18-20]), this is the first study to comprehensively profile miRNA expression in tissue from the two most common histological grades of OV-induced ICC and single most common histological subtype of OV-induced ICC. The miRNA expression profiles were established by microarray analysis on FFPE accessed from the tumor registry at the Liver Fluke and Cholangiocarcinoma Research Center, Khon Kaen, Thailand and the George Washington University (GWU) Medical Center using the following samples: (1) histologically confirmed intrahepatic cholangiocarcinoma tumor tissue (CTT); (2) histologically normal tissue distally macrodissected from the observed dysplasia or frank carcinoma from the same FFPE block as the CTT described above (Distal Normal Tissue or D-NT); and (3) histologically normal non-tumor tissue from individuals undergoing gastric bypass surgery (normal non-tumor tissue or N-NT). We hypothesize that miRNA dysregulation is associated not only with ICC, but also with the histological grade or the subtype of ICC and, may be informative for early diagnosis, prognosis, and patient planning for ICC.

Materials and Methods

Study Samples

Formalin fixed paraffin embedded (FFPE) liver sections from histologically confirmed *O. viverrini* induced ICC archived at the Liver Fluke and Cholangiocarcinoma Research Center, Faculty of Medicine, Khon Kaen University, Thailand were studied. The tumor samples and their corresponding distal non-tumor sections were derived from liver resections performed in the course of palliative treatment for confirmed cases of *O. viverrini*-associated ICC at the Khon Kaen University's Srinagarind Hospital, Khon Kaen, Thailand. In addition, non-tumor controls were derived from livers of 13 individuals (N-NT) from biopsies taken prior to gastric bypass surgery at the George Washington University Medical Center (GWUMC), Washington D.C. to assess baseline liver histology in individuals suspected of severe steatosis or steatohepatitis. The 13 control individuals (N-NT) included 11 females and two males with an average age of 45 years (95% Confidence Interval of 38 to 54 years of age). Clinico-pathological information and representative images of the tissues used in this study are presented in Table 1 and in Figure 1.

Both the Khon Kaen University and GWU IRB determined that the samples used in this study did not meet the definition of human subjects research; i.e., a living individual about whom an investigator conducting research obtains: a) data through intervention or interaction with the individual or b) private identifiable information. This determination was made since the samples were limited to pre-existing, de-identified specimen analysis labeled with a random code.

RNA isolation

A master slide consisting of a 5µm section from the FFPE block was prepared and stained with Harris's hematoxylin and eosin (H&E). Normal (D-NT), necrotic, and tumor tissue (CTT) regions were identified for each sample, and subsequently used as a template for additional microtome sections (8 x 5µm for each case). RNA was isolated from FFPE sections using the miRNeasy

FFPE kit (Qiagen) according to manufacturer's protocol[21]. Total RNA was eluted in 30 µl RNase-free water. The concentration, purity and integrity of the RNA were determined by spectrophotometry (Nanodrop 1000) and with the Agilent 2100 Bioanalyzer/Agilent RNA 6000 Nano Kit and Agilent Small RNA kit. Purified RNA was stored at -80°C.

Microarray Analysis

MicroRNA expression was profiled on the Agilent human miRNA microarray (miRBase Release 16.0) between the following groups (1) ICC tumor tissue (CTT) (n = 16) and a corresponding non-tumor tissue distally macrodissected from the observed dysplasia or frank carcinoma from the same FFPE block from the same ICC tumor block (D-NT) (n = 15) (note case B91 did not contain corresponding non-tumor distal tissue); (2) CTT and normal non tumor-tissue (N-NT) (n = 13) from biopsies of individuals undergoing gastric bypass surgery at GWU; and (3) among the three common histological grades of OV-induced ICC: well differentiated (n = 6), moderately differentiated (n = 2), and papillary tumor (n = 8).

Tissue from CTT, D-NT, and N-NT were equally distributed across six microarrays to prevent bias of the signals to a single microarray. RNA was labeled with Cyanine 3-pCp using Agilent miRNA labeling and hybridization kits and hybridized to the Agilent human miRNA array and scanned. The feature intensities were transferred to digital data using Feature Extraction (V.10.7) software, along with hierarchical clustering [Agilent Gene Spring and Feature Extraction (V.10.7)] (Figure 2A). A sample of papillary tumor (a CTT sample) was excluded from analysis due to a low CC (correlation coefficient) value (<0.7). CC values of the other pairs ranged from 0.7 to 1. During analysis of these data, inter-sample variance was normalized using 90 percentile normalization strategies. Hierarchical Clustering by Pearson correlation and Euclidean distance enabled clustering of samples with similar miRNA profiles, as well as enabling visualization of combinations of miRNAs with similar profiles across the different groups. Differences among groups were statistically compared using one way Analysis of Variance (ANOVA), unpaired Student's *t*-test, and fold change analysis with correction for

multiple testing (Benjamini & Hochberg or BH correction). *P* values of ≤0.05 were considered to be statically significant.

Microarray data was prepared according to MIAME standards and deposited in the GEO (Gene Expression Omnibus Database, National Center for Biotechnology Information, U.S. National Library of Medicine, Bethesda, MD) under accession number GSE53992.

Quantitative Reverse Transcription PCR (qPCR)

cDNA was generated from 250 ng total RNA using the miScript RT II kit (Qiagen) according to the manufacturer's protocol. qPCR was performed (in duplicate) using a Bio-Rad (Hercules, CA) iCycler iQ5 with miScript SYBR Green PCR Kit (Qiagen) with miScript Primer Assays (Qiagen) for controls and six selected miRNAs: miR--135b, -141, -200c, -21, -221, -222. Initial activation was completed at 95℃ for 15 minutes followed by 40 cycles of denaturation, 15 sec, 94℃; annealing, 30 sec, 55℃; and extension, 30 sec, 70℃, followed by a melting curve analysis for 81 cycles at 55℃ and 20 sec dwell time. C_t values were exported and analyzed using SABiosciences tool (http://pcrdataanalysis.sabiosciences.com/mirna) and relative quantitation performed using the $\Delta\Delta C_t$ method [22].Normalization was accomplished using SNORD68 and SNORD95.

RESULTS

Cases and Controls

Detailed clinicopathological characteristics of the ICC FFPE samples used in this study are shown in Table 1 and Figure 1. In brief, FFPE consisted of anonymously coded FFPE from histopathologically confirmed cases of ICC after informed consent from patients who underwent hepatectomy at Srinagarind Hospital, Khon Kaen University and were stored under Best Practices at the Liver Fluke and Cholangiocarcinoma Center, Khon Kaen University, Khon Kaen Thailand, where eligibility into this biorepository requires prior (positive sera or plasma) or current (fecal exam) evidence of infection with *O. viverrini*. The classification system used to

define the tumor growth characteristics of each sample in Table 1 were derived from The Liver Cancer Study Group of Japan [2]and identified tumors as [1] mass-forming, [2] periductal-infiltrating, and [3] intraductal-growing types (Table 1). The Tumor Node and Metastasis (TNM) categories and the staging were derived from the American Joint Committee on Cancer Staging Manual (6^{th} Edition) [23].

Histological grading was done as described by the International Agency for Research on Cancer (IARC) [1]. In brief, assignment of well-differentiated adenocarcinoma to a tumor sample required that 95% of the tumor contain glands. For moderately differentiated, 40 to 94% of the tumor was composed of glands [1] (Figure 1). (Though neither poorly differentiated or undifferentiated carcinomas were used in this study, they would have to display between 5 to 39% of the tumor containing glands or less than 5% of glandular structures, respectively [1].) In the case of papillary type ICC, we followed the IARC classification for tumors of the gallbladder and extrahepatic bile ducts [1], with the lesions having to consist predominantly of papillary structures lined by cells with a biliary phenotype, with good demarcation and consisting of papillary structures lined by tall columnar cells [1] (Figure 1).

Purified RNA exhibited 260/280 and 260/230 Optical Density (OD) ratios of ~2.0 and ~1.9, respectively, indicating that it was pure, and suitable for downstream application. The Agilent 2100 BioAnalyzer (data not shown) was utilized to evaluate the quality of purified RNA. RIN scores ranged from two to three for the samples and 28S and 18S ribosomal RNAs peaks were largely absent, together indicative of degradation of the RNA. RNA in FFPE is expected to be both modified and degraded due to the formalin and duration of storage [13, 24]. However, because of their small size, miRNAs are more stable than other RNA species and have reliably been purified from FFPE [13, 24]. Given the stability of miRNAs in FFPE tissue [25]and reports from other groups and us [26]that low RIN scores have negligible effect on miRNA profiles, the RNA was considered suitable for further analysis.

Tumors and corresponding distal non-tumor tissue shared distinct miRNA profiles

Hierarchical clustering revealed that the N-NT samples grouped together (red tree lines), while clusters of D-NT (blue) and clusters of CTT (grey) scattered together across the heat map (Figure 2A). This observation was statistically confirmed by ANOVA analyses, which showed that there were fewer differences between the CTT and D-NT than between D-NT and N-NT, indicating that non-tumor tissue adjacent to ICC tumors shared similar miRNA profiles. The 3D Principal Components Analyses (Figure 2B) showed that N-NT samples clustered in a manner distinct from both CTT and their corresponding D-NT samples.

One-way analysis of variance (ANOVA), and Student's *t*-test were also used to compare and identify miRNAs significantly dysregulated among the three histological grades of OV-induced ICC: [1] well differentiated; [2] moderately differentiated, and [3] papillary ICC [1]. The first analysis compared CTT with corresponding D-NT from the same ICC FFPE block (Figure 3A), with a second comparison undertaken between CTT and N-NT (Figure 3B). Each histological subtype of ICC showed a distinct suite of miRNAs, which they shared with the cognate distal non-tumor tissue (Figure 3A): i.e., tissue graded as well differentiated, moderately differentiated, or papillary ICC had discrete miRNA profiles, as did adjacent non-tumor tissue. There were, however, minor overlaps between the histological grades, with eight significantly dysregulated among well differentiated and papillary (hsa-miR-200c-3p, -141-3p, -429, -200a-3p, 200b-3p, -222-3p, -210, and ebv-miR-BART1-5p). Additionally, four significantly dysregulated miRNAs were shared by papillary and moderately differentiated ICC (hsa-miR-122-3p, -122-5p, -885-5p, and -196b-5p).

To determine if a distinctive profile of miRNAs could identify ICC tumor tissue from non-tumor liver tissue, the CTT samples as a single group (not divided by histological grade) were compared with the N-NT samples (liver tissue from individuals undergoing gastric bypass

surgery). Here, 40 miRNAs were dysregulated when ICC tissues were compared to non-cancer liver tissue (Figure 3B). However, of these 40 dysregulated miRNAs, only six were shared among the ICC tumor samples when these ICC samples were grouped by histological grade. These six shared dysregulated miRNAs were used for qPCR validation of the microarray analysis. Notably, the remaining 34 dysregulated miRNAs fell into distinct profiles that were associated with the three histological grades of OV-induced ICC. Hence, in a pattern seen throughout this study, the strongest and universal associations between miRNA dysregulation and ICC tumor were evident among the distinct profiles of dysregulated miRNAs and their association with ICC histological subtype.

Distinct miRNA profiles strongly associated with the histologic grade and subtype of ICC

We also compared CTT miRNA dysregulation without comparison to either histologically normal tissue (N-NT) or corresponding non-tumor distal tissue (D-NT). Sixty-one of the >1,600 miRNAs screened had a p value ≤ 0.05 and a fold change > 2.0 (Table 2). Further investigation revealed that miRNA dysregulation was again unevenly distributed among the histological subtypes, with the kind, quantity and the magnitude of the miRNA dysregulation strongly associated with the histological grade or subtype of the ICC. More specifically, miRNAs were significantly increased in the quantity and the magnitude of their dysregulation in moderately differentiated ICC compared to papillary ICC. A similar increase in number and magnitude of dysregulated miRNAs were observed when papillary ICC was compared to well differentiated ICC (Table 2). In short, well-differentiated ICC showed the lowest miRNA dysregulation among the three histological grades, which likely reflects the phenomenon that, unlike papillary and moderately differentiated ICC, well-differentiated tumors show minimal cytological change and often closely resemble the bile duct tissue from which they arise.

qPCR validated microarray findings

To confirm the microarray findings, we used qPCR to analyze six dysregulated miRNAs (above) shared among tumor tissue (CTT) when compared to normal tissue (N-NT): i.e., hsa-mir-135b, -141, -200c, -21, -221, -222. Dysregulation of expression of these six miRNAs was confirmed by qPCR; for example, when tumor tissue was analyzed against normal tissue (N-NT) (Figure 4), miR-141 showed the highest FC in both qPCR (FC = 371; p = 0.0007) and in the microarray. However, interestingly, the qPCR analysis confirmed the two outstanding trends determined by the microarray profiling (Figure 4 and Supplemental Figure 1). First, the magnitude of miRNA dysregulation was associated with histological subtype (Figure 4 and Supplemental Figure 1), with moderately differentiated tissue exhibiting the highest FC by qPCR for five of the six miRNAs (the exception was miR-21). Second, distal tissue non-tumor tissue (D-NT) again closely resembled proximal tumor (CTT) in the magnitude of miRNA dysregulation (Data not shown).

DISCUSSION

This manuscript represents the first comprehensive miRNA expression profiling of OV-induced ICC by histological grades and subtype, adding to a growing literature on the role of miRNAs in hepatocellular neoplasms [14, 17, 20]. In the current report, RNA was recovered from FFPE [21] and used to screen Agilent miRNA microarrays and, for the first time, miRNA dysregulation has been shown to differentiate between healthy non-tumor liver tissue (N-NT) and three most common histopathological types of OV-induced ICC [1]: well-differentiated, moderately differentiated, and papillary ICC tumor. No shared profile of miRNAs emerged as commonly dysregulated among these common histologic subtypes and grade of OV-induced ICC. In a repeated pattern, moderately differentiated ICC tissue showed both the greatest number and magnitude of miRNA dysregulation, followed by the papillary type of ICC, and then well-differentiated ICC. This trend likely reflects the fact that, by definition, moderately differentiated tumor tissue shows greater cytological changes and has the least resemblance to the bile duct

315 tissue from which the tumor arose. Moreover, the three histological subtypes of OV-induced ICC
316 exhibited distinct miRNA signatures, suggestive of the involvement of specific sets of miRNAs in
317 progression of this tumor. This observation is consistent with findings for HCC [14, 17], where
318 the type, number and magnitude of miRNA dysregulation increase with increasing histological
319 differentiation. Functional studies suggest that the association between miRNA dysregulation
320 and histological subtype derive from miRNA modulation of key cellular processes involved in
321 HCC tumor differentiation [14, 17].

322 Unexpectedly, there was a close similarity in miRNA profiles between tumor tissues (CTT) and
323 adjacent non-tumor (D-NT) tissue macrodissected distant from observed dysplasia or frank
324 carcinoma in the FFPE. These findings confirm our previous findings on ICC [27] where, even
325 in the absence of obvious tumor mass or a differentiation in tissue morphology, genetic changes
326 in nearby non-tumor tissue had already occurred. This is also consistent with the role of
327 miRNAs as messengers of tumor-cell invasion as recently described for breast cancer, where
328 miRNAs and proteins involved in cancer progression were identified in exosomes isolated from
329 breast cancer cell clines [25].

330 When tumor tissues (CTT) were compared to healthy tissue (N-NT), 40 miRNAs were observed
331 to be dysregulated. However, the miRNAs dysregulation in this comparison may reflect the
332 possible differences in the composition of the samples; CTT were biopsied from livers resected
333 to confirm OV-induced ICC and may be enriched for cholangiocytes compared to hepatocytes.
334 In comparison, N-NT were biopsied from individuals preparing to undergo gastric bypass
335 surgery may contain more hepatocytes than cholangiocytes. However, even against this
336 backdrop of miRNA dysregulation possibly attributable to differences in the tissue composition
337 and even ethnicity, [14, 17], the same pattern of miRNA dysregulation was evident: moderately
338 differentiated ICC tissue showed the greatest miRNA dysregulation, followed by the papillary
339 type of ICC tumor, and then well-differentiated ICC tumor tissue.

Only six miRNAs were commonly dysregulated among the three types of ICC when compared to healthy liver tissue by microarray, which we confirmed by qPCR. Moreover, the similarity between tumor tissue and their corresponding non-tumor tissue was also observed for these six miRNAs and validated by qPCR, confirming the possibility of genetic or miRNA alterations in apparently healthy tissue adjacent to dysplastic tissue or frank cancer. Together, these data strongly support the main finding that miRNA dysregulation strongly associates with the histological subtypes of OV-induced ICC and is reflected in nearby non-tumor tissue.

A large number of miRNAs have now been associated with different cancers and the majority of miRNAs identified in this work have been previously associated with cancer. For example, hsa-mir-429 is upregulated in bladder cancer [28] and mirs 200c-3p, 141-3p, 200a-3p, 200b-3p have been identified with gastric esophageal [29], , bladder [28] and breast [30]cancer respectively. Two miRNAs typically associated with liver pathology, miR-885-5p [31] and mir-551b-5p [32] were also significantly dysregulated in ICC tissue versus controls, but also showed clear expression differences in the different grades of tumour. Few miRNAs associated with ICC in this study have not been previously been associated with cancer, but the few that have not, for example miR-593-3p, are therefore potential miRNA markers with specificity for ICC.

The main limitation of this study is the absence of a set of non-malignant cholangiocyte tissues as controls, which are rare. If available, inclusion of normal cholangiocytes would provide a precise baseline for the progression of altered miRNA expression and deliver a more parsimonious miRNA profile associated with ICC subtype. Moreover, as we plan to detect these dysregulated profiles in bodily fluids the need for comparison to cholangiocytes will be reduced. The study also does not also contain functional analyses on the individual miRNAs found to be dysregulated. However, the focus of the study was a comprehensive profiling of dysregulated miRNAs in ICC tumor tissue by histological grade. Such descriptive studies are integral

precursors to qualified, hypothesis-driven studies and can guide future functional studies in OV-induced ICC.

There are important translational implications arising from the findings. As recently noted by Rizvi and Gores [33], ICC poses unique diagnostic and prognostic challenges due to its "paucicellular nature, anatomic location, and silent clinical character", requiring a "high index of suspicion" and a "multidisciplinary approach" to diagnosis that involves clinical, laboratory, endoscopic, and radiographic analyses. We add to this multidisciplinary approach miRNA-profiling indicative of histopathological grade. As the aggressiveness of ICC has been strongly associated with the degree of histological differentiation [34], miRNAs indicative of histological differential that are easily accessible in bodily fluids may increase their role in this multidisciplinary approach for ICC as they can be detected earlier and limit the invasive procedures referred to above. Currently, as ICC presents late during the disease, confirmatory needle aspiration biopsy or liver resection (hepatectomy) is required for the type of sample analyzed in this manuscript. However, if these dysregulated miRNAs could be detected in an accessible biofluid(s) (e.g., plasma, sera, urine, etc.) in persons with "a high index of suspicion" prior to liver resection, our findings offer an opportunity for early determination of type of ICC, which could aid in proper treatment. As ICC is highly vascularized, with a propensity for angiogenesis, there is a good probability that these dysregulated miRNAs circulate in the blood. Hence, our ultimate objective is to target these dysregulated miRNA profiles in plasma or sera for screening. Additionally, recent finding of circulating exosomes (or micro vesicles) "laden" with miRNAs secreted from the bile duct of individuals with ICC offers intriguing possibilities for miRNA trafficking and may be responsible for our observation of similarly dysregulated miRNA profiles in apparently normal tissue distal (D-NT) to paired tumors [35]. We plan to investigate miRNAs circulating in bodily fluids as well as their trafficking by exosomes in future studies. In

addition, we also plan to explore the presence of novel miRNAs (not in miBAse 16) by untargeted profiling of these same ICC tissues by RNA Seq.

Finally, as we were able to detect sets of dysregulated miRNAs associated with different CCA subtypes of ICC, we plan to perform functional analyses to decipher the roles of these particular miRNAs in the process of tumor differentiation, including both overexpression and knock-down experiments mediated by antagomirs and/or miRNA sponges [36]. The effect of these genetic manipulations would be evaluated at the phenotypic level, i.e. proliferation, migration assays, etc., and also at the gene expression level [19]. These approaches could advance our understanding in miRNAs in CCA oncogenesis and tumor biology, and advance therapeutic strategies for this infection-related cancer.

ACKNOWLEDGEMENTS

The contents are solely the responsibility of the authors and do not represent the official views of NIAID, NCI, the Katzen Cancer Research Center of the George Washington University, or the NHMRC of Australia. This research was partially supported by awards R01CA155297 (JMB, JPM, and PJB) from the National Cancer Institute, P50AI098639 (BS, JMB, and PJB) from the National Institute of Allergy and Infectious Disease, fellowship support (JPM) and research support (JMB and JPM) from the National Health and Medical Research Council of Australia, and research support from the Dr. Cyrus And Myrtle Katzen Cancer Research Center at the George Washington University (PJB and JMB). Microarrays were hybridized and scanned at the Genomics and Epigenomics Shared Resource, Georgetown University Medical Center with the assistance of David Goerlitz. We would like to thank Dr. Norman Lee, GWU for guidance and advice on microarrays.

411

412 **REFERENCES**

413 [1] Xi Y, Nakajima G, Gavin E, Morris CG, Kudo K, Hayashi K, et al. Systematic analysis of
414 microRNA expression of RNA extracted from fresh frozen and formalin-fixed paraffin-
415 embedded samples. RNA 2007;13:1668-1674.

416 [2] The general rules for the clinical and pathological study of primary liver cancer. The
417 Japanese Journal of Surgery 1989;19:98-129.

418 [3] Khan SA, Thomas HC, Davidson BR, Taylor-Robinson SD. Cholangiocarcinoma. Lancet
419 2005;366:1303-1314.

420 [4] Sripa B, Bethony JM, Sithithaworn P, Kaewkes S, Mairiang E, Loukas A, et al.
421 Opisthorchiasis and Opisthorchis-associated cholangiocarcinoma in Thailand and Laos.
422 Acta Trop 2011;120 Suppl 1:S158-168.

423 [5] Sripa B, Kaewkes S, Sithithaworn P, Mairiang E, Laha T, Smout M, et al. Liver fluke
424 induces cholangiocarcinoma. PLoS Med 2007;4:e201.

425 [6] IARC. Schistosomes, Liver Flukes and Helicobacter Pylori: Internatinal Agency for
426 Research on Cancer World Health Organization; 1994.

427 [7] Cavalli F. Cancer in the developing world: can we avoid the disaster? Nature clinical
428 practice Oncology 2006;3:582-583.

429 [8] Keiser J, Duthaler U, Utzinger J. Update on the diagnosis and treatment of food-borne
430 trematode infections. Current opinion in infectious diseases 2010;23:513-520.

431 [9] Sripa B. Pathobiology of opisthorchiasis: an update. Acta Trop 2003;88:209-220.

432 [10] Woradet S, Promthet S, Songserm N, Parkin DM. Factors affecting survival time of
433 cholangiocarcinoma patients: a prospective study in Northeast Thailand. Asian Pac J
434 Cancer Prev 2013;14:1623-1627.

[11] Nakajima T, Kondo Y, Miyazaki M, Okui K. A histopathologic study of 102 cases of intrahepatic cholangiocarcinoma: histologic classification and modes of spreading. Human pathology 1988;19:1228-1234.

[12] Nakanuma Y, Sato Y, Harada K, Sasaki M, Xu J, Ikeda H. Pathological classification of intrahepatic cholangiocarcinoma based on a new concept. World journal of hepatology 2010;2:419-427.

[13] Pritchard CC, Cheng HH, Tewari M. MicroRNA profiling: approaches and considerations. Nature reviews Genetics 2012;13:358-369.

[14] Braconi C, Patel T. MicroRNA expression profiling: a molecular tool for defining the phenotype of hepatocellular tumors. Hepatology 2008;47:1807-1809.

[15] Budhu A, Jia HL, Forgues M, Liu CG, Goldstein D, Lam A, et al. Identification of metastasis-related microRNAs in hepatocellular carcinoma. Hepatology 2008;47:897-907.

[16] Karakatsanis A, Papaconstantinou I, Gazouli M, Lyberopoulou A, Polymeneas G, Voros D. Expression of microRNAs, miR-21, miR-31, miR-122, miR-145, miR-146a, miR-200c, miR-221, miR-222, and miR-223 in patients with hepatocellular carcinoma or intrahepatic cholangiocarcinoma and its prognostic significance. Molecular carcinogenesis 2013;52:297-303.

[17] Murakami Y, Yasuda T, Saigo K, Urashima T, Toyoda H, Okanoue T, et al. Comprehensive analysis of microRNA expression patterns in hepatocellular carcinoma and non-tumorous tissues. Oncogene 2006;25:2537-2545.

[18] Chen L, Yan HX, Yang W, Hu L, Yu LX, Liu Q, et al. The role of microRNA expression pattern in human intrahepatic cholangiocarcinoma. Journal of hepatology 2009;50:358-369.

[19] Chusorn P, Namwat N, Loilome W, Techasen A, Pairojkul C, Khuntikeo N, et al. Overexpression of microRNA-21 regulating PDCD4 during tumorigenesis of liver fluke-

associated cholangiocarcinoma contributes to tumor growth and metastasis. Tumour biology : the journal of the International Society for Oncodevelopmental Biology and Medicine 2013;34:1579-1588.

[20] Kawahigashi Y, Mishima T, Mizuguchi Y, Arima Y, Yokomuro S, Kanda T, et al. MicroRNA profiling of human intrahepatic cholangiocarcinoma cell lines reveals biliary epithelial cell-specific microRNAs. Journal of Nippon Medical School = Nippon Ika Daigaku zasshi 2009;76:188-197.

[21] Plieskatt JL, Rinaldi G, Feng Y, Levine PH, Easley S, Martinez E, et al. Methods and matrices: approaches to identifying miRNAs for Nasopharyngeal carcinoma. Journal of translational medicine 2014;12:3.

[22] Livak KJ, Schmittgen TD. Analysis of relative gene expression data using real-time quantitative PCR and the 2(-Delta Delta C(T)) Method. Methods 2001;25:402-408.

[23] Cancer AJCo. AJCC Cancer Staging Manual, 6 ed. Philadelphia: Lippincott Raven Publishers; 2002.

[24] Mayr M, Zampetaki A, Willeit P, Willeit J, Kiechl S. MicroRNAs within the continuum of postgenomics biomarker discovery. Arteriosclerosis, thrombosis, and vascular biology 2013;33:206-214.

[25] Kruger S, Abd Elmageed ZY, Hawke DH, Worner PM, Jansen DA, Abdel-Mageed AB, et al. Molecular characterization of exosome-like vesicles from breast cancer cells. BMC cancer 2014;14:44.

[26] Jung M, Schaefer A, Steiner I, Kempkensteffen C, Stephan C, Erbersdobler A, et al. Robust microRNA stability in degraded RNA preparations from human tissue and cell samples. Clinical chemistry 2010;56:998-1006.

[27] Weinbren K, Mutum SS. Pathological aspects of cholangiocarcinoma. The Journal of pathology 1983;139:217-238.

[28] Han Y, Chen J, Zhao X, Liang C, Wang Y, Sun L, et al. MicroRNA expression signatures of bladder cancer revealed by deep sequencing. PloS one 2011;6:e18286.

[29] Zang W, Wang Y, Du Y, Xuan X, Wang T, Li M, et al. Differential expression profiling of microRNAs and their potential involvement in esophageal squamous cell carcinoma. Tumour biology : the journal of the International Society for Oncodevelopmental Biology and Medicine 2014;35:3295-3304.

[30] Kolacinska A, Morawiec J, Fendler W, Malachowska B, Morawiec Z, Szemraj J, et al. Association of microRNAs and pathologic response to preoperative chemotherapy in triple negative breast cancer: preliminary report. Molecular biology reports 2014.

[31] Gui J, Tian Y, Wen X, Zhang W, Zhang P, Gao J, et al. Serum microRNA characterization identifies miR-885-5p as a potential marker for detecting liver pathologies. Clin Sci (Lond) 2011;120:183-193.

[32] Liu P, Xia L, Zhang W-l, Ke H-j, Su T, Deng L-b, et al. Identification of serum microRNAs as diagnostic and prognostic biomarkers for acute pancreatitis. Pancreatology.

[33] Rizvi S, Gores GJ. Pathogenesis, diagnosis, and management of cholangiocarcinoma. Gastroenterology 2013;145:1215-1229.

[34] Nakanuma Y, Sasaki M, Ikeda H, Sato Y, Zen Y, Kosaka K, et al. Pathology of peripheral intrahepatic cholangiocarcinoma with reference to tumorigenesis. Hepatology research : the official journal of the Japan Society of Hepatology 2008;38:325-334.

[35] Li L, Masica D, Ishida M, Tomuleasa C, Umegaki S, Kalloo AN, et al. Human bile contains microRNA-laden extracellular vesicles that can be used for cholangiocarcinoma diagnosis. Hepatology 2014.

[36] Sun W, Julie Li YS, Huang HD, Shyy JY, Chien S. microRNA: a master regulator of cellular processes for bioengineering systems. Annual review of biomedical engineering 2010;12:1-27.

513

514 **TABLES**

Table 1. Clinicopathological characteristics of 16 *O. viverrini* associated ICC patients used in study.

ID	Sex	Age	OV Status	Ethnicity	Histological grade	Gross Classification	TNM	Staging
B070	M	61	Positive	Asian	WD	Mass-forming	T3N0M0	IIIA
B079	M	61	Positive	Asian	WD	Periductal infiltrating, invasive intraductal and mixed	T4N1M0	IIIB
B083	F	53	Positive	Asian	WD	Mass-forming	T3N0M0	IIIA
B099	M	48	Positive	Asian	WD	Mass-forming	T3N0M0	IIIA
Y042	M	61	Positive	Asian	WD	Mass-forming	T3N1M0	IIIC
B091	M	63	Positive	Asian	MD	Periductal infiltrating, invasive intraductal and mixed	T4N1M0	IIIB
Y070	F	63	Positive	Asian	MD	Mass forming	T3N0M0	IIIA
Y056	F	56	Positive	Asian	PC	Periductal infiltrating, invasive intraductal and mixed	T4N1M0	IIIB
Y062	M	57	Positive	Asian	PC	Periductal infiltrating, invasive intraductal and mixed	T4N1M0	IIIB
B049	M	64	Positive	Asian	PC	Mass forming	T3N0M0	IIIA
Y083	F	51	Positive	Asian	PC	Mass forming	T3N1M0	IIIC
Y088	F	58	Positive	Asian	PC	Periductal infiltrating, invasive intraductal and mixed	T4N1M0	IIIB
Y089	F	60	Positive	Asian	PC	Mass forming	T3N1M0	IIIC
Y093	M	63	Positive	Asian	PC	Periductal infiltrating, invasive intraductal and mixed	T4N1M0	IIIB
Y096	F	64	Positive	Asian	PC	Mass forming	T3N1M0	IIIC

M = Male; F = Female

Histological types: tumor differentiation: WD = Well Differentiated tubular adenocarcinoma; MD = Moderately Differentiated tubular adenocarcinoma; and PC = Papillary Carcinoma

Staging: Tumor Node Modular Classification and Staging from AJCC Sixth edition [23]

515

Table 2. Statistically significant miRNAs by ANOVA among histological grades of ICC. p(corr) < 0.05, FC > 2 in at least two conditions, and raw values >30. FC over 5 is highlighted gray.

		Fold Change		
miRNA	**p (Corr)**	**Moderate vs. Papillary**	**Moderate vs. Well**	**Papillary vs. Well**
hsv1-miR-H5-5p	0.012487	-2.63889	2.5606	6.75720
hsa-miR-122-3p	0.015622	-101.23811	-29.61597	3.41836
hsa-miR-885-5p	0.029224	-25.07646	-9.7333	2.57634
hsa-miR-122-5p	0.012487	-24.25102	-9.4541	2.56512
hsa-miR-593-3p	1.29E-04	-3.28851	-1.321101	2.48921
hsa-miR-3150b-3p	6.26E-04	-2.29151	-1.12618	2.03474
hsa-miR-3615	0.01371	-3.34746	-2.13974	1.56442
hsa-miR-141-5p	0.027995	24.48213	37.49911	1.53169
hsv1-miR-H3	1.45E-04	-4.75690	-3.18933	1.49150
ebv-miR-BART1-5p	1.09E-05	-33.84535	-24.5516	1.37854
hcmv-miR-UL70-3p	0.001715	-2.77372	-2.01710	1.37501
hsa-miR-670	5.30E-04	-11.33349	-8.45322	1.34073
hsa-miR-610	5.30E-04	-2.646281	-2.01362	1.31419
hsa-miR-139-3p	0.002508	-2.791654	-2.13508	1.30751
hsa-miR-195-3p	2.06E-04	-3.170986	-2.58510	1.22664
hsa-miR-7-5p	0.043624	6.330076	7.72615	1.22055
hsa-miR-4279	4.82E-05	-3.101136	-2.70097	1.14816
hsv2-miR-H7-3p	1.45E-04	-2.313273	-2.02378	1.14304
ebv-miR-BART11-3p	4.82E-05	-2.980643	-2.61500	1.13982
hsa-miR-605	0.001945	-2.701080	-2.41566	1.11815
hsv1-miR-H1	0.002834	-2.904213	-2.61325	1.11134
hsa-miR-1915-5p	5.30E-04	-2.852665	-2.56942	1.11024
hsa-miR-125b-2-3p	0.002592	-2.216214	-2.00739	1.10402
hsa-miR-551b-5p	5.53E-04	-2.957645	-2.71326	1.09007
hsa-miR-1909-5p	0.01109	-2.187650	-2.01615	1.08506
hsa-miR-29b-3p	0.023843	3.098345	3.36130	1.08487
hsa-miR-454-3p	0.002592	2.045415	2.20069	1.07592
hsa-miR-3155a	1.46E-04	-2.152257	-2.01079	1.07035
hsa-miR-132-3p	0.00401	2.678988	2.85432	1.06545
kshv-miR-K12-12	0.020011	-2.531076	-2.46680	1.02606
hsa-miR-181a-5p	0.029224	2.180832	2.22445	1.02000

hsa-miR-3151	5.30E-04	-2.134066	-2.09751	1.01742
hsa-miR-93-5p	0.041808	2.233950	2.17524	-1.02699
hiv1-miR-H1	0.044691	-2.210104	-2.30172	-1.04146
hsa-miR-4317	0.026188	2.105246	2.01773	-1.04337
hsa-miR-27a-3p	0.043624	2.826095	2.69947	-1.04690
hsa-miR-141-3p	0.013427	10.81161	10.23016	-1.05684
hsa-miR-21-5p	0.020011	3.79329	3.56598	-1.06374
hsa-miR-331-3p	0.002612	3.12259	2.87675	-1.08546
hsa-miR-23a-3p	0.041377	3.13897	2.81030	-1.11695
hsa-miR-3065-5p	0.012487	-2.18501	-2.45883	-1.12532
hsa-miR-4267	0.004431	-2.03989	-2.33321	-1.14380
hsa-miR-200c-3p	0.018654	11.08151	9.62122	-1.15178
hsa-miR-146b-5p	0.012487	4.02472	3.46128	-1.16278
hsa-miR-106b-5p	0.029224	2.88392	2.45642	-1.17403
hsa-miR-210	0.014745	4.13911	3.39742	-1.21831
hsa-miR-425-5p	0.012487	3.40384	2.76990	-1.22887
hsa-miR-222-3p	0.004354	5.95207	4.82987	-1.23234
hsa-miR-221-3p	0.003211	5.83729	4.68405	-1.24620
hsa-miR-135b-5p	0.020011	30.41217	22.75650	-1.33642
hsa-miR-665	0.034674	-2.04905	-2.75661	-1.34531
hsa-miR-223-3p	0.011902	5.21594	3.65900	-1.42550
hsa-miR-1273c	0.011902	-2.04719	-3.03805	-1.48401
hsv1-miR-H8*	0.023843	-2.12146	-3.40951	-1.60716
hsa-miR-183-5p	0.03395	7.25323	4.29224	-1.68985
hsa-miR-132-5p	0.020011	26.20608	15.16595	-1.72795
hsa-miR-31-5p	1.09E-05	117.31276	60.36202	-1.94349
hsa-miR-3152-3p	0.01109	-8.38224	-16.99140	-2.02710
hsa-miR-182-5p	0.023843	49.70194	20.06405	-2.47716
hsa-miR-221-5p	0.012907	76.10488	30.66719	-2.48163
hsa-miR-31-3p	1.09E-05	1992.38980	742.40680	-2.68369

FIGURES

Fig. 1. Representative images of CTT, D-NT, and N-NT FFPE tissue. Panel A: normal liver with mild macrovesicular steatosis *(arrowhead)* and portal triad *(arrows),* H&E (20X). Panel B: a trichrome stain shows no significant pericentral fibrosis; a normal amount of periportal fibrous tissue is present *(arrow)* H&E (2X). Panel C: well differentiated cholangiocarcinoma as shown by angulated glands with luminal mucin *(long arrow)* and cytologic atypia *(short arrow)* in a dense fibrous stroma, H&E (20X). Panel D: moderately differentiated cholangiocarcinoma, with malignant cribriform glands involving a nerve (*short arrow*) and a lymphatic space (*arrowhead*), H&E (10X). Panel E: invasive component of papillary adenocarcinoma composed of angulated glands with luminal mucin, H&E (20X); Panel F: invasive papillary adenocarcinoma *(arrow)* and interface with adjacent normal liver *(*)*, H&E (10X).

Fig. 2. Hierarchical Analysis and clustering of FFPE cholangiocarcinoma and healthy liver samples by microarray. (A) Healthy liver samples (N-NT) show a hierarchical profile clustered together (Red), while tumor (CTT) (Grey) and distal apparently normal tissue macrodissected distant from dysplasia or frank cancer (D-NT) (Blue) show some diversity, but clustered closely with (CTT). The >1600 human miRNAs are also hierarchical grouped (Left) and expression exhibited on a heatmap. **(B)** PCA 3D clustering of cholangiocarcinoma and healthy liver FFPE cohorts**.** (N-NT) tissue from non-CCA cases cluster together, while tissue samples from CCA cases showed diversity in overall scoring.

Fig. 3. Histological bias of miRNA analysis from microarray. miRNAs were analyzed by two methods according to histology: (A) Distal tissue from the same CCA patient (D-NT) compared to CCA tumor tissue (CTT) and (B) CTT compared against non-tumor samples biopsied from of individuals undergoing gastric bypass surgery (N-NT). miRNAs that exhibited (A) FC ≥ 2, $p \leq 0.05$, and raw values >30 via a paired test, and (B) FC ≥ 2, $p \leq 0.05$, raw values > 30 via unpaired T test, were used in the comparison lists.

Fig. 4. miRNA Fold Changes between CCA histological classifications by qPCR. Six miRNAs (hsa-mir: -135b, -141, -200c, -21, -221, -222) identified by microarray were verified by qPCR in the same CTT, N-NT and D-NT(not shown) samples. The qPCR results were also compared to fold changes determined by microarray (Supplemental Figure 1). Error bars represent 95% confidence interval, and asterisks denote p-value: (*) $p \leq 0.05$ and (**) $p \leq 0.01$, (***) $p \leq 0.001$.

SUPPLEMENTAL FIGURES

Supplementary Fig. S1. miRNA Fold Changes between qPCR and Microarray by CCA histological classifications. Fold changes of six miRNAs (hsa-mir: -135b, -141, -200c, -21, -221, -222) verified by qPCR and compared to values determined during microarray analysis of the same samples.

Figure 1

Fig. 1.

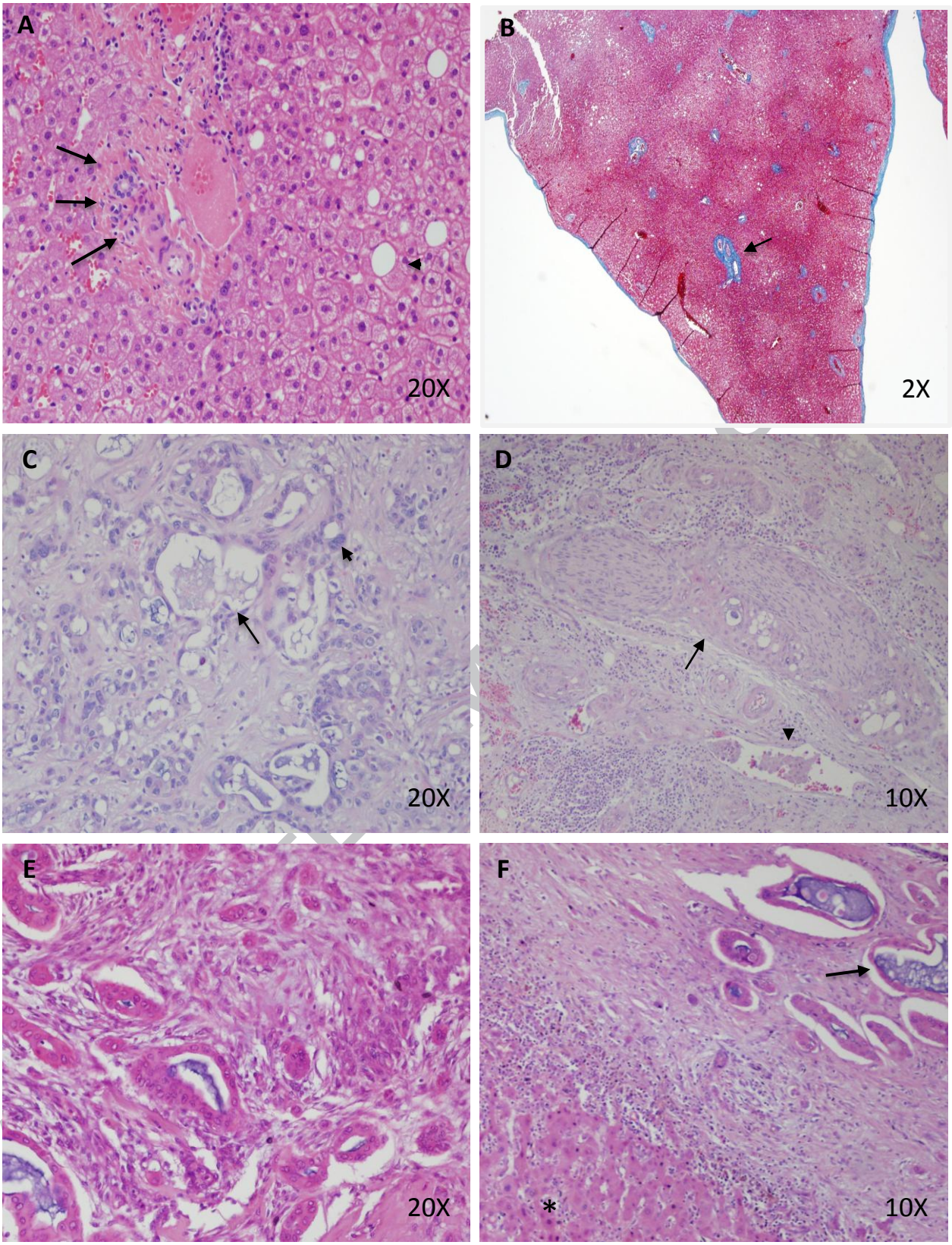

Figure 2

Fig. 2.

A

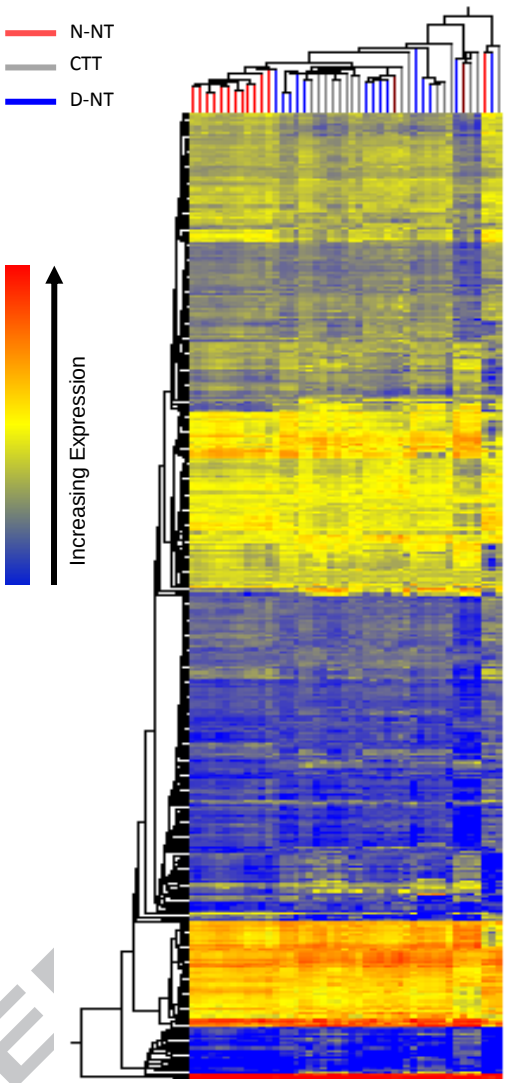

B

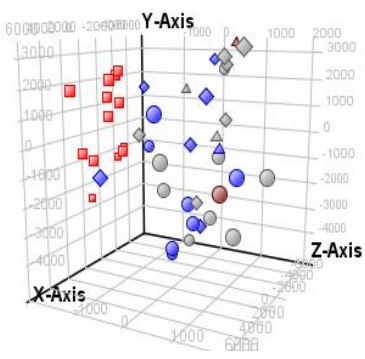

N-NT
D-NT
Necrosis (Not analyzed)
CTT

N-NT
CTT-Moderately Differentiated
CTT-Papillary Carcinoma
CTT-Well Differentiated

Figure 3
Fig. 3.

A

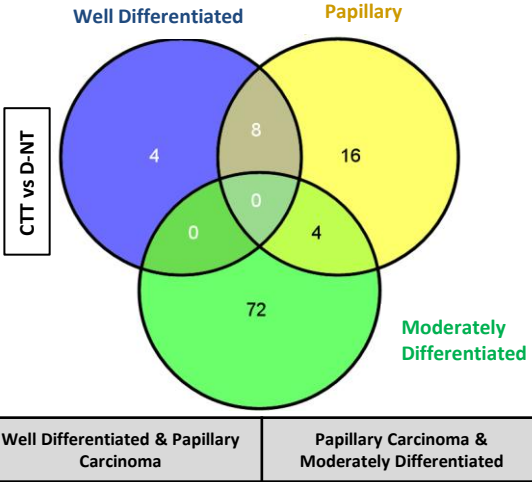

Well Differentiated & Papillary Carcinoma	Papillary Carcinoma & Moderately Differentiated
hsa-miR-200c-3p hsa-miR-141-3p hsa-miR-429 hsa-miR-200a-3p hsa-miR-200b-3p hsa-miR-222-3p hsa-miR-210 ebv-miR-BART1-5p	hsa-miR-122-3p hsa-miR-122-5p hsa-miR-885-5p hsa-miR-196b-5p

B

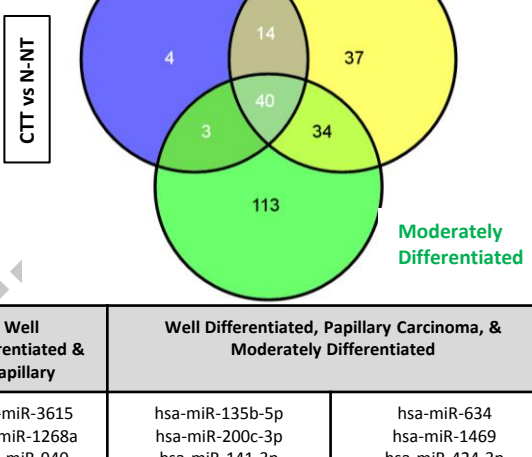

Well Differentiated & Papillary	Well Differentiated, Papillary Carcinoma, & Moderately Differentiated	
hsa-miR-3615 hsa-miR-1268a hsa-miR-940 hsv2-miR-H10 hsa-miR-3665 hsa-miR-3188 hsa-miR-2110 hsa-miR-2861 hsa-miR-373-5p hsa-miR-3187-3p hsa-miR-1915-3p hsv1-miR-H17 hsv1-miR-H3 hsa-miR-1280	hsa-miR-135b-5p hsa-miR-200c-3p hsa-miR-141-3p hsa-miR-200a-3p hsa-miR-222-3p hsa-miR-21-3p hsa-miR-200b-3p hsa-miR-221-3p hsa-miR-21-5p hsa-miR-34b-5p hsa-miR-4281 hsa-miR-181c-5p hsa-miR-34a-5p hsa-miR-3656 hsa-miR-125a-5p hsa-miR-181b-5p hsa-miR-23a-5p hsv1-miR-H2* hsa-miR-30c-1-3p hsa-miR-3945	hsa-miR-634 hsa-miR-1469 hsa-miR-424-3p hsa-miR-193b-5p hsa-miR-1261 hsa-miR-513a-5p hsa-miR-671-3p hsa-miR-3654 hsa-miR-1258 hsa-miR-513b hsa-miR-1275 kshv-miR-K12-5* hsa-miR-629-3p hsa-miR-3936 hsa-miR-516a-5p hsa-miR-3921 hsa-miR-3666 kshv-miR-K12-7* ebv-miR-BART1-5p hsa-miR-4309

Fig. 4.